Experimental Analysis of a Double Swirl Burner

F. Cozzi*, F. Motta*, F. Cobianchi*, L. Zampini*, A. Francabandiera*
fabio.cozzi@polimi.it
*Department of Energy, Politecnico di Milano, Via Lambruschini 4, 20156 Milano, Italy

Abstract
The increasingly stringent regulations push towards the developments of industrial combustion systems (boilers, furnaces, and gas turbine) having single digit NOx emission. A well-known methodology to achieve high combustion efficiency and low pollutants emission in combustion system is the use of both swirling flows and staged combustion.
This work reports preliminary experimental results obtained on a research burner exploiting both swirl and radially staged combustion air. The burner has been developed at Politecnico di Milano, it is composed by two coaxial co-rotating swirling jet; an inner premixed jet and an outer swirling air flow. The swirl level of the outer jet can be regulated independently form that of the inner one. Experimental results evidence the swirl level of the premixing jet strongly affects the isothermal flow field structure, the pollutant emissions and flame stability. The burner operates with low NOx emissions, anyhow a non-monotonic trend is evidenced by both CO and NOx emissions when varying the equivalence ratio (i.e. the swirl level) of the premixed jet. Further experimental analysis is required to improve the burner design and to define the best operating conditions.

Introduction

A well-known methodology to achieve high performances in gas turbine combustor and burners is the use of swirling flows. The recirculation region originated by these flows improves mixture formation, promote flame stabilization, reduces flame length and reduce pollutant emissions [1-5]. Besides, pollutant emissions can be further reduced by using the staged combustion concept [6-9].
In a previous work a staged burner using non-swirled premixed injectors were tested; both radial and axial injection into the secondary swirled air were investigated [9]; results evidenced reduced NOx emissions and not negligible CO emissions [9]. The primary objective of this research project is to further investigate the staged combustion concept by using a new premixed injector. The latter is of swirl-type, and fuel/primary air premixing occurs just upstream of the exit section, so to avoid flashback issues. Preliminary experimental results about flame stability, pollutant emissions and flame structure are reported.

Experimental Set-up

Experimental tests are performed on a pilot-scale swirl burner and using natural gas as fuel. The set-up is composed by an octagonal combustion chamber (80 mm by side and 290 mm in height) connected to a double co-rotating swirling burner

having a bottle-shaped structure, Figure 1(a). The fuel and the primary air are injected by a swirl premixed injector, the latter is composed by two concentric pipes ending into a cup injection head; primary air and fuel flow in the inner and outer pipe, respectively, see Figures 1(b) and 2. The injector is designed in such a way that mixing of primary air and fuel occurs just upstream of the exit section, so to avoid flashback issues. The secondary air flows in the gap between the premixed injector and the inner wall of the swirl generator, Figure 1(b). More details can be found in [10]-[11]. Swirl is generated in both the secondary air and in the premixed jet by using a tangential plus axial flow injection; the swirl direction is the same for the two coaxial jets (i.e. they are co-rotating).

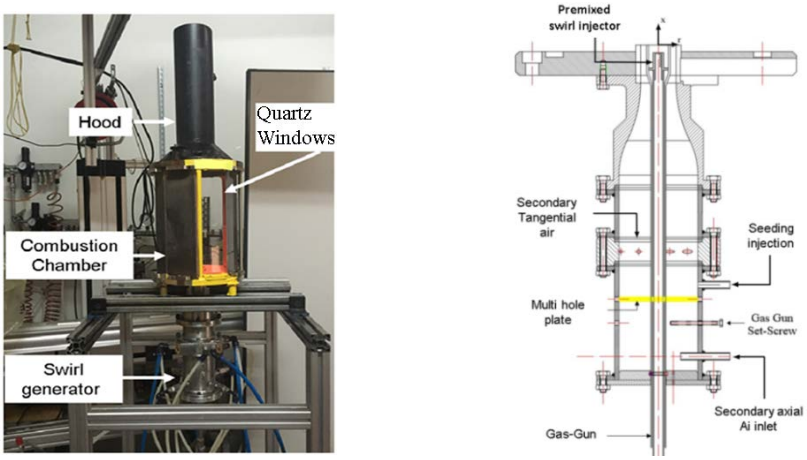

(a) (b)

Figure 1. (a) Photo of the burner. (b) Sketch of the swirl generator and of the premixed swirl injector.

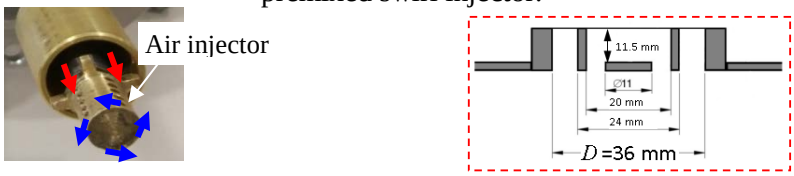

(a) (b)

Figure 2. (a) Swirl premixed injector, the air injector is extracted from the cup injection head to show it. (Blue arrows: air. Red arrows: fuels). (b) detail of swirl generator exit section.

The exit section of the swirl burner has an inner diameter $D = 36$ mm, while the outer diameter of the premixed injector is $d_{op} = 24$ mm and its inner diameter is $d_{ip} = 20$ mm, Figure 2(b). The Reynolds number, $Re = (\rho V_{bulk} D) / \mu$, is based on the nozzle diameter, D, the bulk mean velocity, V_{bulk}, and the dynamic air viscosity, μ. The bulk velocity is computed as the total volumetric flow rate (total air+fuel) divided by the area of the exit section, i.e. $\pi D^2/4$. Split ratios of the secondary air, SR_s, and of the premixed jet, SR_p, are defined according to

equations (1). The split ratio quantify the fraction of the mass flow rate injected tangentially; thus their value set the swirl level imposed to each jet.

$$SR_p = \dot{m}_{ap}/(\dot{m}_f + \dot{m}_{ap}) \qquad SR_s = \dot{m}_{atg,s}/(\dot{m}_{atg,s} + \dot{m}_{aax,s}) \qquad (1)$$

Where $\dot{m}_{ap}$, $\dot{m}_{atg,s}$ and $\dot{m}_{aax,s}$ are the mass flow rates of the premixing air, of the secondary tangential air and of the secondary axial air, respectively; while $\dot{m}_f$ is the fuel mass flow rate. We introduce a global fuel to air equivalence ratio, Φ_g, based upon the measured mass flow rates of the fuel (natural gas) and of the total air (i.e. $\dot{m}_{atg,s} + \dot{m}_{aax,s} + \dot{m}_{ap}$), and a premixed equivalence ratio, Φ_p, based on the mass flow rates of the fuel and the primary air, see equations (2).

$$\Phi_g = \frac{1}{f_{stech}} \frac{\dot{m}_f}{\dot{m}_{atg,s} + \dot{m}_{aax,s} + \dot{m}_{ap}} \qquad \Phi_p = \frac{1}{f_{stech}} \frac{\dot{m}_f}{\dot{m}_{ap}} \qquad (2)$$

In the premixed injector the air is injected tangentially and the fuel axially, Figure 2; thus the premixed equivalence ratio and the split ratio of the premixed stream cannot be varied independently. The relationship between Φ_p and SR_p is given by equation (3) and shown in Figure (3). Being the natural gas almost composed by methane, we assume $f_{stech} = 9.52$.

$$\Phi_p = \frac{1}{f_{stech}} \frac{1 - SR_p}{SR_p} \qquad (3)$$

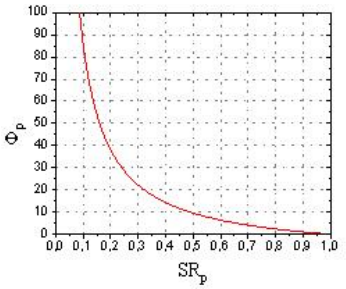

Figure 3. Φ_p vs. SR_p, values computed using equation (3), $f_{stech} = 9.52$.

Stereo Particle image velocimetry (Stereo-PIV) is employed to characterise the near field flow patterns under non-reacting conditions. More details on the PIV system are reported in [10]. Still photographs of the flames are also taken to document the large variations of flame morphology and to compare with the PIV maps.

The burner is operated at atmospheric pressure and nominal inlet gas temperature of 300 K, in overall lean conditions ($\Phi_g \cong 0.6$), with input thermal power of $\approx 12 - 16$ kW and swirl numbers $S \approx 1.3$. All mass flow rates are controlled by thermal mass flow meter with 1% accuracy. A stainless steel probe, mounted on a cylindrical extension of the conical hood, extracts flue gas to measure the global emission performance of the burner. The probe is connected to a Testo 360 gas analyzer to measure CO, CO_2, O_2 and NOx emissions.

Isothermal flow field

The structure of the isothermal flow field in the mid plane of the burner were investigated by means of Stereo-PIV. Despite in combustion condition the flow field could change due to the heat release from the flame, this analysis provides a first useful information about the effect of SR_p. Tests were carried out using air in place of the fuels, so to simulate the burner operating at a fixed thermal power of 16 kW and at a fixed $\Phi_g \cong 0.6$. Both the total flow rate and SR_s are kept constant and ≅445 Nl/min and 0.5, respectively; while three different values of the primary split ratio are used: $SR_p = 0, 0.72$ and 0.86. When changing SR_p, the secondary air is reduced so as to keep the total flow rate constant. At 20 °C the operating conditions correspond to a $V_{bulk} \cong 7.8\ m/s$ and $Re \cong 20000$.

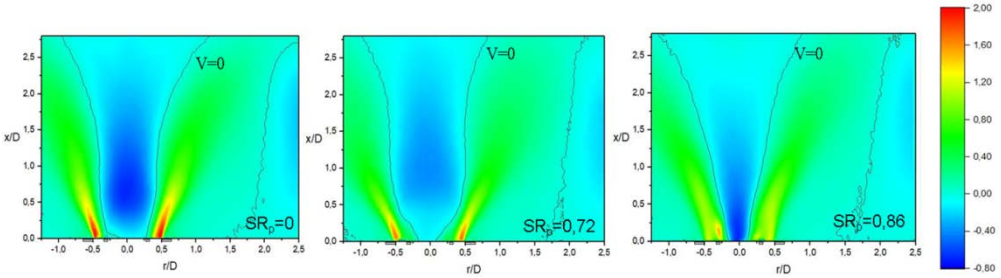

(a) (b) (c)

Figure 4. Normalized axial velocity V/V_b.The black line shows iso-line $V/V_b = 0$.

The isothermal mean flow field evidence an almost axisymmetric structure along with a stable vortex breakdown under all the investigated conditions. Size and location of the recirculating zone are affected by SR_p. By increasing SR_p both the swirl level and the momentum of the inner jet increases; this at first weakens and pushes slightly downstream the central recirculation zone, Figure 4(b). Then, at $SR_p = 0.86$, the inner jet rules the flow field, the vortex breakdown moves upstream and its width shrink. A similar effect of SR_p (i.e. of the premixed equivalence ratio Φ_p) on the flow field is evoked for combustion condition by observing the flame shape, see next section.

Flame stability and flame geometry

Blow off conditions are investigated using two different approaches. In the first one, the air flow rates are all kept constant while the fuel flow rate is slowly reduced until flame blow off occurs. The smallest fuel flow rate before blow-off is taken as the blow-off limit. In the second one, the secondary air is increased until blow-off occurs; the primary air flow rate, the fuel flow rate, SR_p and SR_s are all kept constant. The highest secondary air flow rate before flame blow-off is taken as the blow-off limit. For both approaches the starting condition are shown in Table 1. The experimental results evidence that by reducing the thermal power blow-off occurs at much leaner conditions as compared to increasing the secondary air,

compare Figure 5(a) and 5(b). The primary air flow rate results to affect the flame shape, while the fuel flow rate mainly affects the flame size. On the other side at fixed SR_s the secondary air has only a minor effect on both flame shape and size, see insets in Figure 5(b).

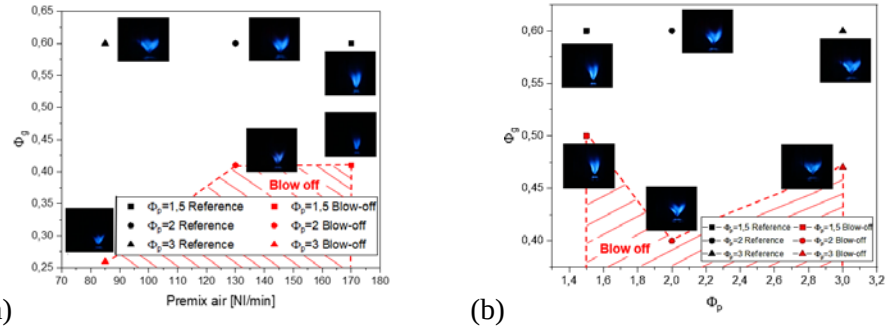

(a) (b)

Figure 5. Flame stability. (a) Blow-off boundary by reducing fuel flow rate. (b) Blow-off boundary by increasing secondary air. For all cases $SR_s = 0.5$

Table 1. Starting condition for blow-off tests, for all cases $\Phi_g \cong 0.6$.

		$\Phi_{premix} = 1.5$	$\Phi_{premix} = 2$	$\Phi_{premix} = 3$
Fuel flow rate	[Nl/min]	26.8 (16 kW)	26.8 (16 kW)	26.8 (16 kW)
Premix air flow rate	[Nl/min]	170	128	85
Secondary tang. air	[Nl/min]	130	150	170
Secondary axial air	[Nl/min]	130	150	170

NOx and CO Emissions

Emission indexes of NOx and CO, measured at $\Phi_g = 0.6$; 0.8, $SR_s = 0.5$ and $P_{th} = 12$ kW, are shown in Figure 6(a)-(b), their values are generally low. At $\Phi_p = 8$ the flame has an asymmetric shape and impinges on the combustor wall, at the impinging site flame quenching occurs, likely this justify the higher CO emission and lower NOx emission observed at that premixing ratio. By decreasing the global equivalence ratio Φ_g from 0.8 to 0.6 the NOx emission decreases while the CO ones increases.

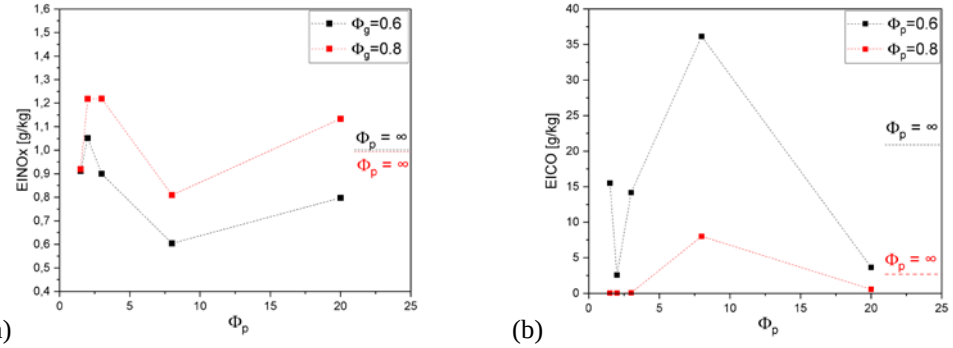

(a) (b)

Figure 6. (a) EINOx. (b) EICO. For all cases $SR_s = 0.5$ and $P_{th} = 12$ kW.

Conclusions

A preliminary analysis of a research burner exploiting both swirl and radially staged combustion air has been carried out. The burner features a double coaxial swirl injector; a central premixed and swirling jet is coaxially injected into an outer swirling air jet. Due to the injector configuration, the equivalence ratio and the split ratio (i.e. swirl level) of the central premixed jet cannot be varied independently. Stereo-PIV measurements, performed under isothermal conditions, evidence a strong influence of the swirled premixed jet on the flow field. The burner is able to operate at very lean condition when the central jet is strongly swirled (i.e Φ_p=1.5). Pollutant emissions are generally low; nevertheless at Φ_p=8 the asymmetric flame, likely generated by the burner aerodynamics, impinges on the burner wall increasing CO emission. Further experimental analysis is required to improve the burner design and to define the best operating conditions.

References

[1] Gupta A.K., Lilley D.G., Syred N., *Swirl flows*, Abacus Press, 1984.

[2] Claypole T.C., Syred N., "The effect of swirl burner aerodynamics on NOx formation", Proc. Comb. Inst. 18:81-89 (1981).

[3] Cheng T.S., Chao Y.-C., Wu D.-C., Yuan T., Lu C.-C., Cheng C.-K., "Chang J.-M., Effects of fuel-air mixing on flame structures and NOx emissions in swirling methane jet flames", Proc. Comb. Inst. 27:1229-1237 (1998).

[4] Olivani A., Solero G., Cozzi F., Coghe A., "Near field flow structure of isothermal swirling flows and reacting non-premixed swirling flames", Exp. Therm. Fluid. Sci., 31(5) (2007) 427-436.

[5] Cozzi F., Coghe A., Sharma R., "Analysis of local entrainment rate in the initial region of isothermal free swirling jets by Stereo PIV", Exp. Therm. Fluid. Sci., 94 (2018) 281-294.

[6] Cheng T. S., Chao Y. C., Wu D. C., Hsu H. W., Yuan T., "Effects of partial premixing on pollutant emissions in swirling methane jet flames". Combust. Flame, 125(1-2) (2001) 865-878.

[7] Kim S.K., Breikin T.V., Hargrave S.M., Thompson H.A., Fleming P.J., Riley S.J., "Staged combustion control for aviation engines: a multi-objective optimization approach", IFAC Proc. Volumes 35.1, Spain (2002): 265-270.

[8] Straub D.L., Casleton K.H., Lewis R.E., Sidwell T.G., Maloney D.J., Richards G.A., "Assessment of rich-burn, quick-mix, lean-burn trapped vortex combustor for stationary gas turbines", J. Eng. Gas Turbines Power 127 (2005) 36–41.

[9] Cozzi F., Coghe A., "Effect of air staging on a coaxial swirled natural gas flame", Exp. Therm. Fluid. Sci., 43 (2012) 32–39.

[10] Francabandiera A., Zampini L., "Experimental and numerical analysis of a double swirl burner under isothermal conditions", Politecnico di Milano (2018).

[11] Marcelli J., "Caratterizzazione sperimentale di un bruciatore parzialmente premiscelato a doppio swirl alimentato a GN", Politecnico di Milano (2016).